

Tunable Dielectric Resonators with Dielectric Tuning Disks

Tao Shen, *Student Member, IEEE*, Kawthar A. Zaki, *Fellow, IEEE*, and Chi Wang, *Senior Member, IEEE*

Abstract—Tunable dielectric resonators with dielectric tuning disks in cylindrical and rectangular enclosures are modeled by mode matching method. Tuning properties of TE_{01} mode such as tuning ranges, spurious mode separation, unloaded quality factors, couplings, etc., are investigated for both rod- and ring-type dielectric resonators. Wide tuning ranges are obtained while other properties of resonators are maintained over the tuning ranges.

Index Terms—Dielectric resonators.

I. INTRODUCTION

Dielectric resonators are widely used in microwave components such as filters and oscillators. In some applications, tunability of resonant frequency is required. Metallic tuning screws might be employed, but their tuning ranges are limited. This is intuitive since in dielectric resonators, most electromagnetic fields are confined in the resonators of high dielectric constants. Metallic tuning screws are more appropriate for fine tuning. Wide tuning ranges could be achieved by using metallic tuning disks. However, this will deteriorate unloaded quality factors of resonators. Dielectric tuning disks can provide wide tuning ranges, and meanwhile avoid the degradation of unloaded quality factors.

In [1] and [2], tunable dielectric resonators with metallic tuning screws or disks are investigated using finite-element method. Tunable dielectric resonators composed of two identical dielectric resonators are investigated in [3]–[5]. However, the tuning ranges of the TE_{01} mode of the resonators are limited by the approach of spurious TE_{02} mode, which will be discussed later.

In this paper, tunable dielectric resonators with dielectric tuning disks in cylindrical and rectangular enclosures are modeled by mode matching method. Tuning properties of TE_{01} mode such as tuning ranges, spurious mode separation, unloaded quality factors, couplings, etc., are investigated for both rod- and ring-type dielectric resonators. Wide tuning ranges are obtained while other properties of resonators are maintained over the tuning ranges.

II. MODELING

Generalized dielectric resonators placed in cylindrical and rectangular enclosures are modeled by mode matching method. The motivation of modeling the generalized structure is that varieties of dielectric resonators can be dealt with by using the

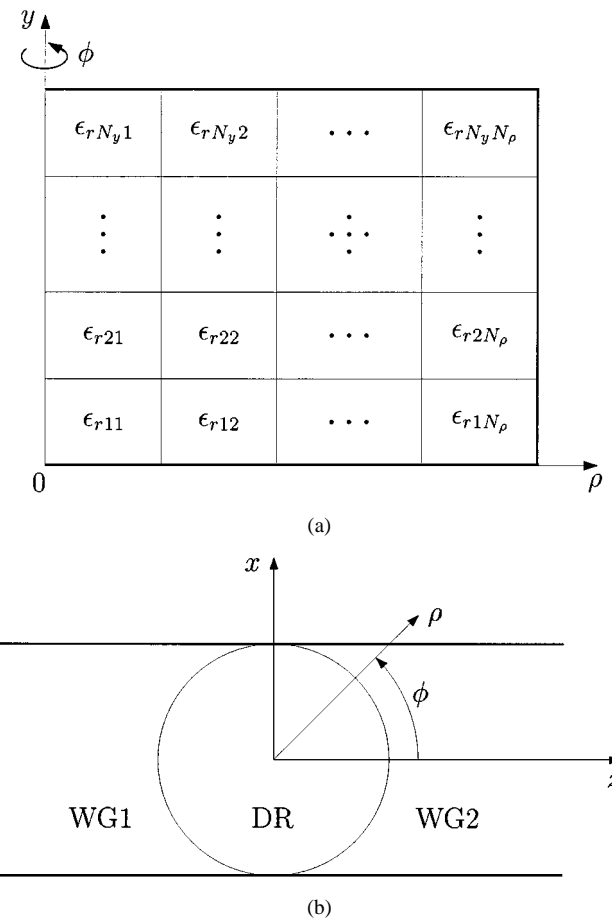


Fig. 1. (a) A generalized dielectric resonator in a cylindrical enclosure. (b) A generalized dielectric resonator loaded waveguide.

structure directly, which eliminates the need of formulation and coding for each specified resonator configuration.

A. Cylindrical Enclosure Case

For the generalized dielectric resonator placed in a cylindrical enclosure, shown in Fig. 1(a), the modeling approach is detailed in [6] and will be outlined here briefly as follows.

The structure is modeled in a cylindrical coordinate system (ρ, ϕ, y) . It is divided into N_ρ radial regions according to its discontinuity along the ρ -axis, and each radial region has N_y layers according to its discontinuity along the y -axis. Each radial region can be viewed as a parallel-plate multilayer radial waveguide. Fields (specifically, the y -directed axial dependence; see the Appendix) in each layer of the parallel-plate multilayer radial waveguide are expressed in terms of trigonometric functions. The characteristic equation is obtained by enforcing field continuity conditions at the interface between two neighboring

Manuscript received March 6, 2000; revised August 22, 2000.

T. Shen and K. A. Zaki are with the Department of Electrical and Computer Engineering, University of Maryland, College Park, MD 20742 USA.

C. Wang is with Radio Frequency Systems Inc., Marlboro, NJ 07746 USA.

Publisher Item Identifier S 0018-9480(00)10771-9.

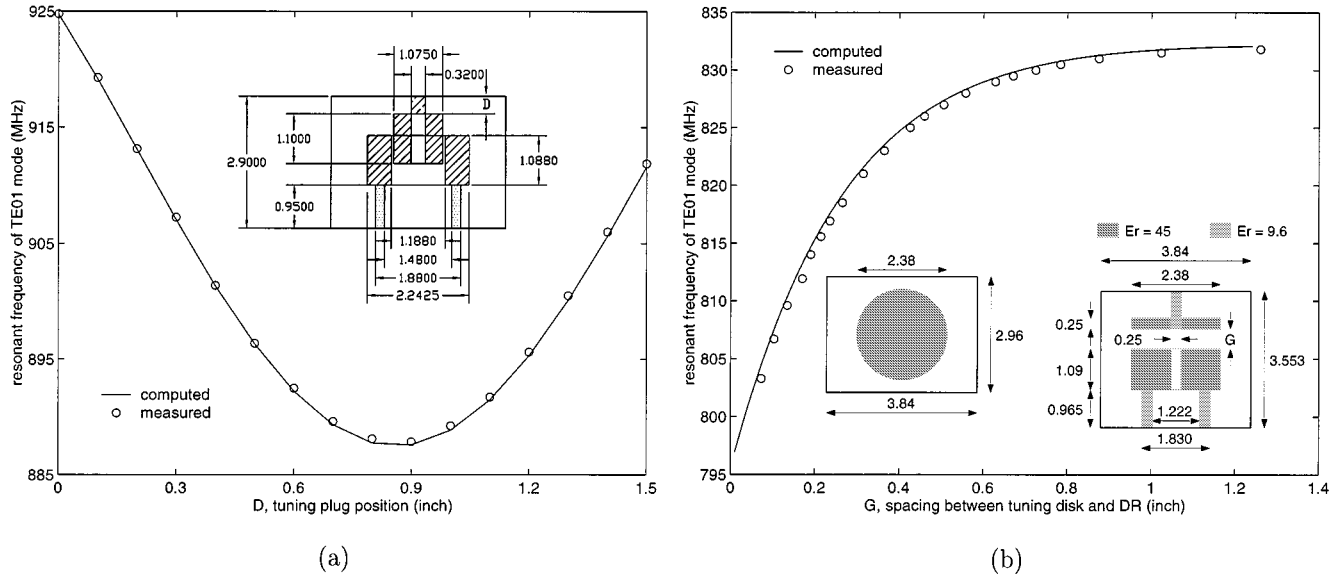


Fig. 2. Comparison between measured and computed tuning frequencies of (a) a dielectric resonator placed in a cylindrical enclosure and (b) a dielectric resonator placed in a rectangular enclosure. Dimensions shown are given in inches. In (a), the enclosure diameter is 3.85 in, and the dielectric constants of the resonator and tuning plug (solid-lined), the support (dotted), and the tuning-plug rod (dash-lined) are 45, 2, and 2.5, respectively.

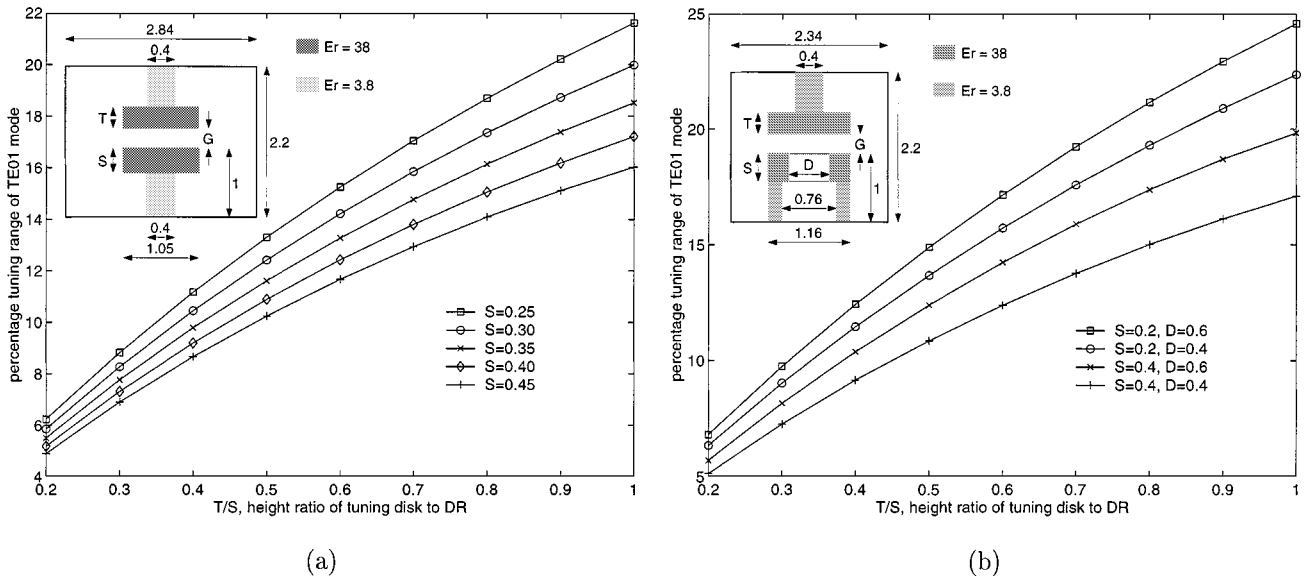


Fig. 3. Percentage tuning ranges of two dielectric resonators. (a) Rod-type resonator. (b) Ring-type resonator. Dielectric resonators are placed in cylindrical enclosures. Dimensions shown are given in inches.

layers successively and dispersion relations. From the characteristic equation, the eigenmode expressions of the parallel-plate multilayer radial waveguide can be determined. The above approach is detailed in the Appendix.

Fields in each radial region are expressed in terms of the eigenmodes of the corresponding parallel-plate multilayer radial waveguide. Enforcing field continuity conditions at the interface and taking proper inner products lead to field coefficient relation equations between two neighboring radial regions. Cascading these field coefficient relation equations successively from the innermost region to the outermost region leads to

$$[\mathbf{M}_C \quad \mathbf{M}_D] \begin{bmatrix} \mathbf{C} \\ \mathbf{D} \end{bmatrix} = \mathbf{0} \quad (1)$$

where \mathbf{C} and \mathbf{D} are the outgoing and ingoing wave coefficient vectors, respectively, of the outermost cylindrical dielectric resonator region and \mathbf{M}_C and \mathbf{M}_D are the cascaded inner product matrices related with \mathbf{C} and \mathbf{D} , respectively.

Enforcing boundary conditions of the side enclosure yields

$$\mathbf{D} = \mathbf{T}\mathbf{C} \quad (2)$$

where \mathbf{T} is the diagonal boundary-condition matrix. Substituting (2) into (1) to eliminate \mathbf{D} or \mathbf{C} , the characteristic matrix for the structure is obtained. Searching for the zeroes of the determinant of the characteristic matrix gives the resonant frequencies. The corresponding field distributions are then obtained by solving the characteristic equation and the field

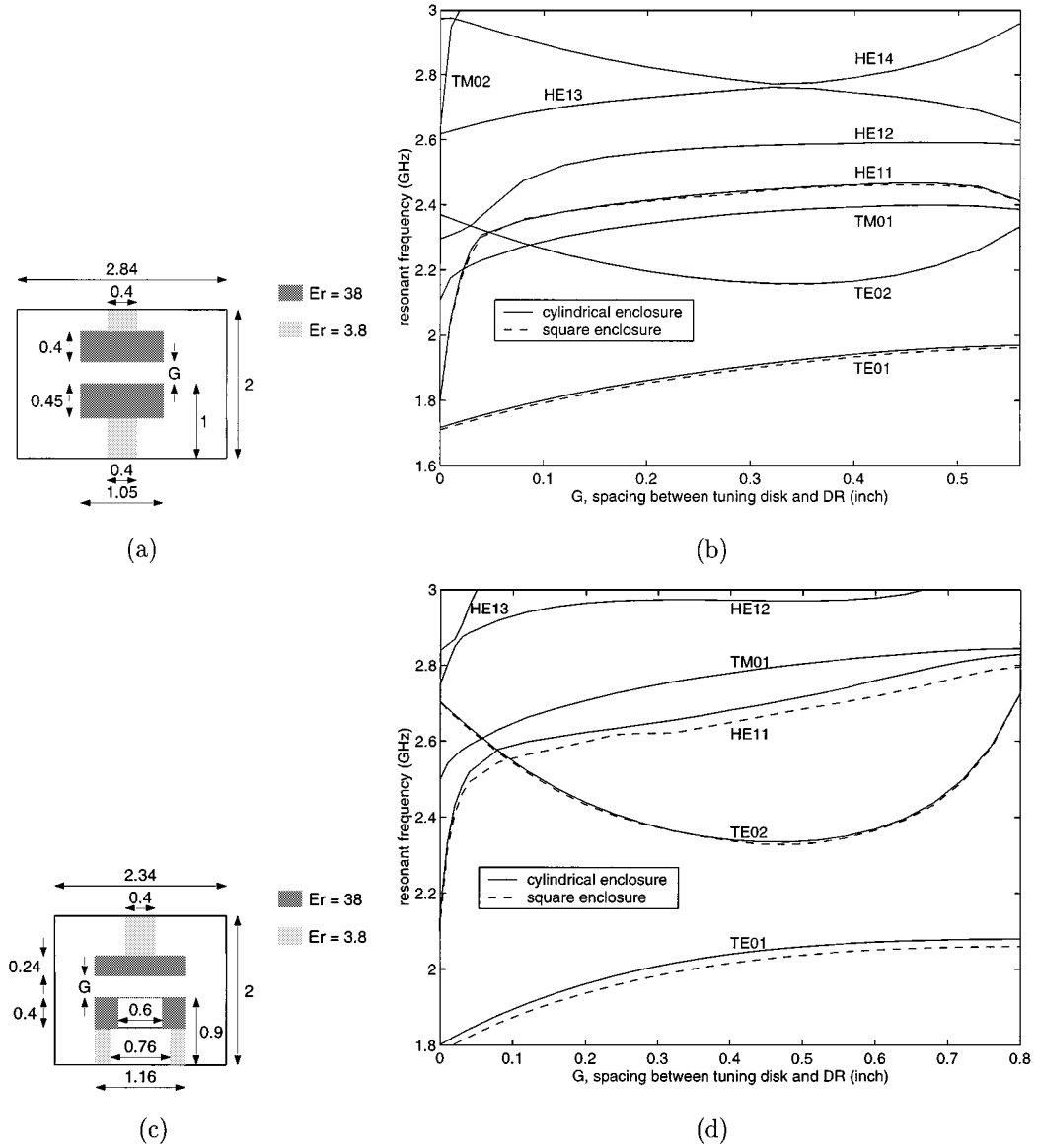


Fig. 4. Mode charts of two dielectric resonators placed in cylindrical enclosures. (a) Dimensions and (b) mode charts of the rod-type resonator. (c) Dimensions and (d) mode charts of the ring-type resonator. Also plotted are resonant frequencies of TE_{01} , TE_{02} , and HE_{11} modes for the square enclosure case. Dimensions shown are given in inches.

coefficient relation equations. From the field distributions, the unloaded quality factors and the couplings between two identical dielectric resonators can be calculated. In the coupling calculation, the improved large-aperture coupling theory with the aperture thickness correction factor taken into account [7], [8] is used. The coupling theory gives quite accurate coupling values [9].

B. Rectangular Enclosure Case

For the generalized dielectric resonator placed in a rectangular enclosure, a generalized dielectric resonator loaded rectangular waveguide shown in Fig. 1(b) is first modeled. It is divided into three regions: the cylindrical dielectric resonator region DR and the rectangular waveguide regions WG1 and WG2. The modeling of the dielectric resonator region is the same as described above for the cylindrical enclosure case. Fields in the

waveguide regions are expressed in terms of the eigenmodes of the rectangular waveguide. Enforcing field continuity conditions at the interface between the dielectric resonator region and the waveguide regions and taking proper inner products lead to the following field coefficient relation equation [10]:

$$\begin{bmatrix} \mathbf{C} \\ \mathbf{D} \end{bmatrix} = [\mathbf{M}_{A1} \quad \mathbf{M}_{A2}] \begin{bmatrix} \mathbf{A}_1 \\ \mathbf{A}_2 \end{bmatrix} + [\mathbf{M}_{B1} \quad \mathbf{M}_{B2}] \begin{bmatrix} \mathbf{B}_1 \\ \mathbf{B}_2 \end{bmatrix} \quad (3)$$

where \mathbf{A}_1 and \mathbf{B}_1 are the incident and reflected wave coefficient vectors, respectively, of the first waveguide region WG1, \mathbf{A}_2 and \mathbf{B}_2 are the incident and reflected wave coefficient vectors, respectively, of the second waveguide region WG2, and \mathbf{M}_{A1} , \mathbf{M}_{A2} , \mathbf{M}_{B1} , and \mathbf{M}_{B2} are the inner product matrices related with the corresponding wave coefficient vectors. Since different coordinate systems are involved in the computation of the inner product matrices, Bessel-Fourier series are used such that all the

inner product integrals can be evaluated analytically [10]. This can improve the efficiency and accuracy of computation.

Substituting (3) into (1) to eliminate \mathbf{C} and \mathbf{D} , the generalized scattering matrix of the generalized dielectric resonator loaded rectangular waveguide is obtained. Shifting the reference plane position of the generalized scattering matrix and short-circuiting it lead to the characteristic equation for the corresponding dielectric resonator in a rectangular enclosure. From the characteristic equation, the resonant frequencies, field distributions, unloaded quality factors, etc., can be obtained. The couplings between two dielectric resonators in rectangular enclosures can also be calculated accurately using the approach described in [9].

Fig. 2 shows the comparison between computed and measured tuning frequencies of TE_{01} mode of two tunable dielectric resonators: one placed in a cylindrical enclosure and the other placed in a rectangular enclosure. The computed results are in good agreement with the measured results for both enclosure cases. For the ring-type resonator shown in Fig. 2(a), a dielectric tuning plug is used.

III. RESULTS AND DISCUSSION

Fig. 3 shows the percentage tuning ranges of TE_{01} mode of rod- and ring-type dielectric resonators. The tuning range increases as the tuning disk becomes thick compared with the height of resonator. For a fixed height ratio of tuning disk and resonator, the tuning range increases with an increased aspect ratio of resonator (the ratio of diameter to height of resonator.) In addition, for the ring-type resonator, the tuning range increases with an increased inner diameter of resonator. Intuitively, as the volume of the tuning disk becomes large compared with the volume of the resonator, the electromagnetic fields are confined in the resonator to a less extent and are easier to disturb by the tuning disk. The results shown in Fig. 3 are obtained for the cylindrical enclosure case. For the square enclosure case, it is found that the results are almost the same as those for the cylindrical enclosure case. Generally speaking, the difference of resonant frequencies between the cylindrical and rectangular enclosures is small for the resonators of high dielectric constants.

Fig. 4 shows the mode charts with respect to the spacing between tuning disk to resonator of rod- and ring-type dielectric resonators placed in cylindrical enclosures. Also plotted are the resonant frequencies of TE_{01} , TE_{02} , and HE_{11} modes for the square enclosure case. Good spurious mode separation from operating TE_{01} mode is observed over the whole tuning ranges. As mentioned above, for the tunable resonator composed of two identical dielectric resonators [5], the tuning ranges of TE_{01} mode are limited. As the spacing between two resonators increases, the resonant frequencies of TE_{01} and TE_{02} (denoted as TEH_{01} and TEE_{01} , respectively, in [5]) modes approach each other (which means the coupling between the two resonators becomes weak.) If dielectric disks are used as tuning elements, their height can be adjusted to avoid the problem. As shown in Fig. 4, as the spacing between tuning disk and resonator increases, the resonant frequency of operating TE_{01} mode rises, while the resonant frequency of TE_{02} mode falls first to some

TABLE I
QUALITY FACTORS OF THE TWO DIELECTRIC RESONATORS OF FIG. 4 PLACED IN CYLINDRICAL ENCLOSURES. G REPRESENTS THE SPACING BETWEEN TUNING DISK AND RESONATOR. Q_u , Q_d , AND Q_c REPRESENT THE UNLOADED TOTAL QUALITY FACTOR, THE QUALITY FACTOR DUE TO DIELECTRIC LOSSES, AND THE QUALITY FACTOR DUE TO (ENCLOSURE) CONDUCTOR LOSSES, RESPECTIVELY. IN COMPUTATION, A LOSS TANGENT OF 1×10^{-4} AND A CONDUCTIVITY OF 15.67×10^5 S/in ARE ASSUMED

G (inch)	rod-type resonator		
	Q_u	Q_d	Q_c
0.04	9833	10255	238684
0.12	9820	10300	210858
0.20	9780	10324	185550
0.28	9719	10333	163661
0.36	9669	10330	150602
0.44	9681	10319	156675
0.52	9773	10305	189322

G (inch)	ring-type resonator		
	Q_u	Q_d	Q_c
0.04	9485	10249	127223
0.16	9491	10318	118362
0.28	9484	10344	114033
0.40	9472	10340	112777
0.52	9473	10323	114932
0.64	9497	10307	120863
0.76	9533	10298	128279

extent and then rises away from the TE_{01} mode. Therefore, good spurious mode separation is maintained over the whole tuning range.

It is also seen from Fig. 4 that the difference of resonant frequencies of TE_{01} , TE_{02} , and HE_{11} modes between the cylindrical and square enclosures is larger for the ring-type dielectric resonator than for the rod-type dielectric resonator (although for both types of resonators, as mentioned above, generally speaking the difference of resonant frequencies between the two kinds of enclosures is small.) For the resonant frequencies of TE_{02} mode of the rod-type resonator, the difference between the two kinds of enclosures is nearly indistinguishable. This is due to the fact that for the rod-type resonator, the size ratio of enclosure to resonator is larger and therefore the enclosure has less effect on the resonance.

Table I gives the quality factors of TE_{01} mode of the two dielectric resonators of Fig. 4 placed in cylindrical enclosures. Over the whole tuning range, Q_d (the quality factor due to dielectric losses) is almost unchanged, while Q_c (the quality factor due to conductor losses) is kept one order greater than Q_d . Therefore, high Q_u (the unloaded total quality factor) is maintained over the whole tuning ranges. On the contrary, for the metallic tuning disks, it is imaginable that as the tuning disk approaches the dielectric resonator, Q_c decreases steadily to be on the same order as or even less than Q_d , and therefore Q_u is deteriorated.

Figs. 5 and 6 show the couplings (through rectangular windows between two identical resonators) of the two dielectric resonators of Fig. 4 placed in cylindrical and square enclosures, respectively. It is seen that the couplings are mainly determined by the slot dimensions and maintained well over the most tuning

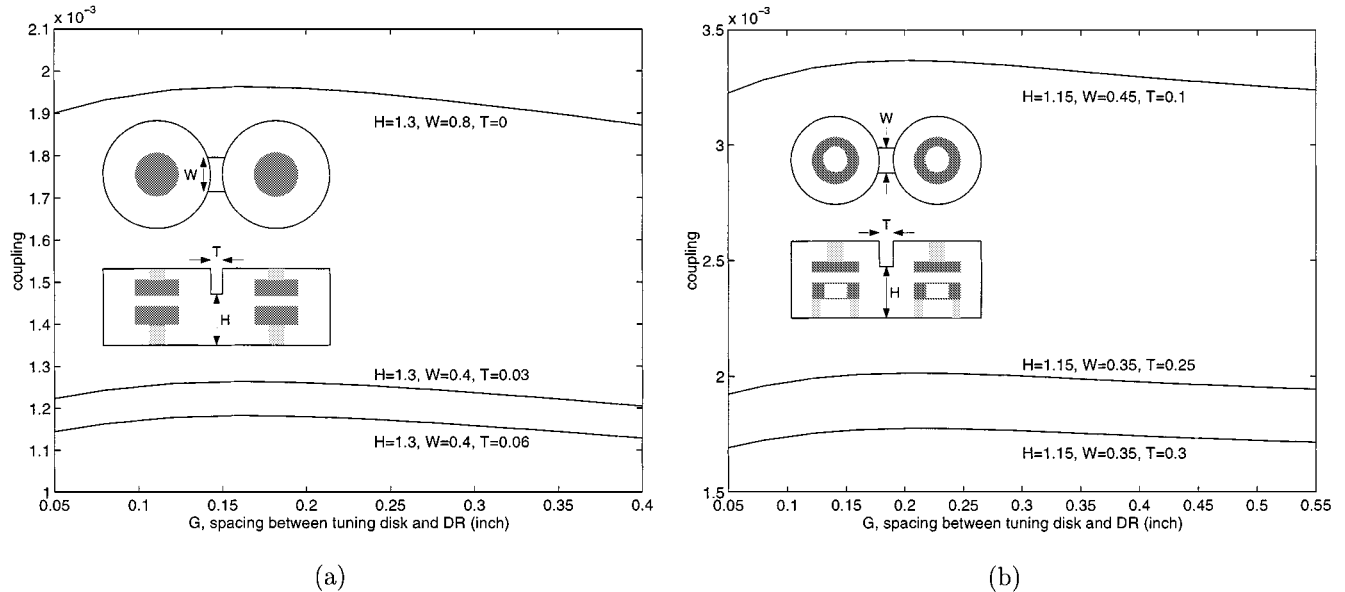


Fig. 5. Couplings of the two dielectric resonators of Fig. 4 placed in cylindrical enclosures. (a) Rod-type resonator. (b) Ring-type resonator. Dimensions shown are given in inches.

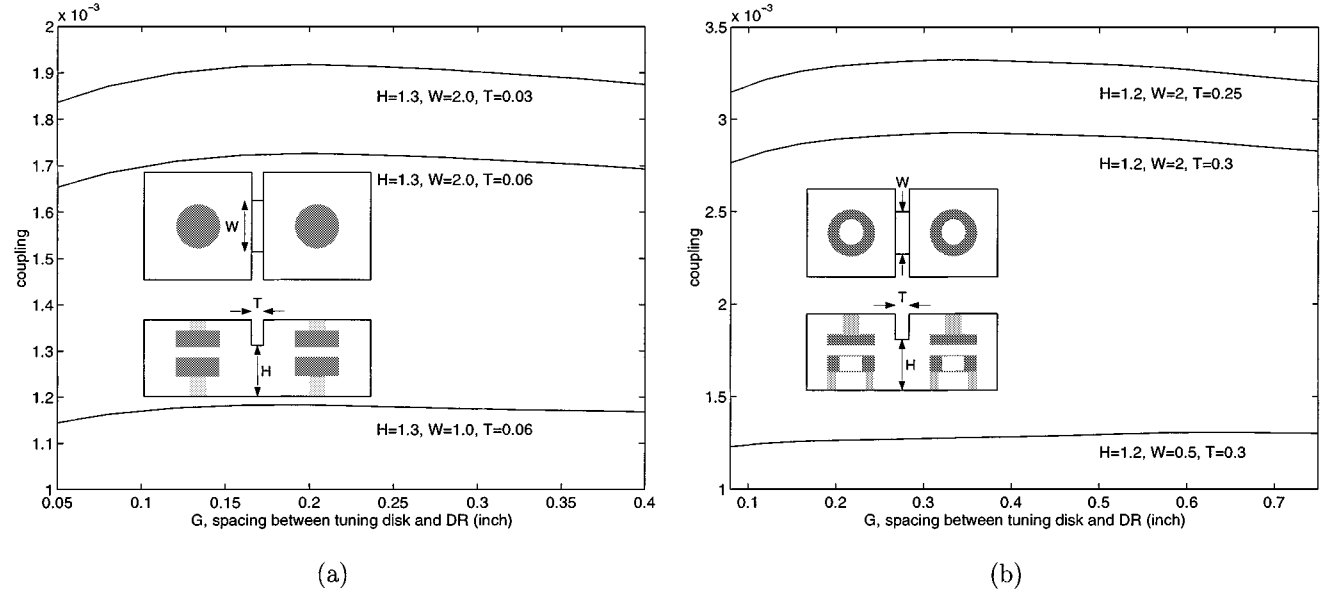


Fig. 6. Couplings of the two dielectric resonators of Fig. 4 placed in square enclosures. (a) Rod-type resonator. (b) Ring-type resonator. Dimensions shown are given in inches.

ranges. Therefore, filters composed of these resonators can be tuned without touching coupling screws.

IV. SUMMARY

Tunable dielectric resonators with dielectric tuning disks in cylindrical and rectangular enclosures are modeled by mode matching method. Tuning properties of TE_{01} mode such as tuning ranges, spurious mode separation, unloaded quality factors, couplings, etc., are investigated for both rod- and ring-type dielectric resonators. Dielectric tuning disks can be used to provide wide tuning ranges while other properties of resonators are maintained over the tuning ranges.

APPENDIX PARALLEL-PLATE MULTILAYER RADIAL WAVEGUIDES

The parallel-plate multilayer radial waveguide is shown in Fig. 7. It is composed of arbitrary N layers of dielectric constant of ϵ_{ri} and height d_i ($i = 1, 2, \dots, N$). The eigenmodes of the radial waveguide can be categorized into TE and TM modes with respect to the z -axis. For TE modes, $E_z = 0$, and the remaining field components can be derived from the axial magnetic field H_z , while for TM modes, $H_z = 0$, and the remaining field components can be derived from the axial electric field E_z . The solution of the scalar (H_z for TE modes or E_z for TM modes) wave equation in cylindrical coordinates is a product of

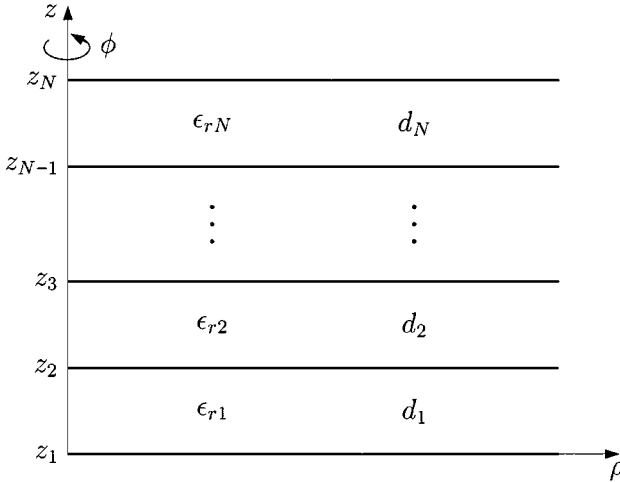


Fig. 7. A parallel-plate multilayer radial waveguide.

three terms: the radial dependence $R(\rho)$, the azimuthal dependence $Q(\phi)$, and the layer-related axial dependence $Z_i(z)$.

The radial and azimuthal dependencies that apply for all the layers are of the form

$$R(\rho) = C_n J_n(\xi\rho) + D_n Y_n(\xi\rho) \quad (4)$$

and

$$Q(\phi) = \begin{cases} \sin(n\phi) \\ \cos(n\phi) \end{cases} \quad (5)$$

respectively, where J_n and Y_n are Bessel functions of first and second kind, respectively, and of order n ; ξ is the radial (ρ -directed) wavenumber; and C_n and D_n are the field coefficients.

The axial dependence $Z_i(z)$ of the i th layer is

$$Z_i(z) = A_i \frac{\sinh[\gamma_i(z - z_i)]}{\gamma_i} + B_i \cosh[\gamma_i(z - z_i)] \quad (6)$$

where A_i and B_i are the unknown field coefficients to be determined later and γ_i is the axial (z -directed) wave number of the i th layer. For TE modes, B_1 and B_N vanish, whereas A_1 and A_N vanish for TM modes.

The axial wave number γ_i of the i th layer are related with each other through the dispersion relation

$$\xi^2 = k_i^2 + \gamma_i^2 \quad (7)$$

where $k_i^2 = k_0^2 \epsilon_{r(i)}$ is the wavenumber of the i th layer (k_0 is the free-space wavenumber) and, as mentioned above, ξ is the radial wave number that applies for all the layers.

Enforcing field continuity conditions [6] at the interface ($z = z_i$) between two neighboring layers successively yields the recursive relations of the field coefficients A_i and B_i of the i th layer with each other

$$\begin{bmatrix} A_{i+1} \\ B_{i+1} \end{bmatrix} = \mathbf{M}_i(d_i) \begin{bmatrix} A_i \\ B_i \end{bmatrix}, \quad i = 1, 2, \dots, N-2 \quad (8)$$

$$\mathbf{M}_{i+1}(-d_{i+1}) \begin{bmatrix} A_{i+1} \\ B_{i+1} \end{bmatrix} = \mathbf{M}_i(d_i) \begin{bmatrix} A_i \\ B_i \end{bmatrix}, \quad i = N-1 \quad (9)$$

where

$$\mathbf{M}_i(d_i) = \begin{bmatrix} \cosh(\gamma_i d_i) & \gamma_i^2 \frac{\sinh(\gamma_i d_i)}{\gamma_i} \\ \frac{\sinh(\gamma_i d_i)}{\gamma_i} & \cosh(\gamma_i d_i) \end{bmatrix} \quad (10)$$

for TE modes, while TM modes have the same $\mathbf{M}_i(d_i)$ except that the second-row entries are multiplied by a factor of $\epsilon_{r(i)}/\epsilon_{r(i+1)}$.

Cascading the above field coefficient relations from the first layer to the last layer successively, and noting that B_1 and B_N vanish for TE modes, whereas A_1 and A_N vanish for TM modes, lead to the characteristic equation. For TE modes, the characteristic equation is

$$\left| \begin{array}{c|c} \text{left column of} & \text{left column of} \\ \overbrace{\mathbf{M}_N(-d_N)}^{\text{left column of}} & \overbrace{\prod_{i=1}^{N-1} \mathbf{M}_i(d_i)}^{\text{right columns}} \\ \hline & \end{array} \right| = 0. \quad (11)$$

2x2 determinant

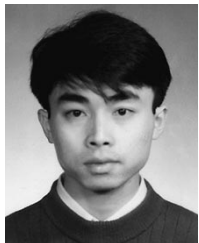
The characteristic equation for TM modes is the same as that above except that the right columns of $\mathbf{M}_N(-d_N)$ and $\prod_{i=1}^{N-1} \mathbf{M}_i(d_i)$ constitute the 2×2 determinant. Searching for the zeroes of the characteristic equation gives the axial wave number γ_i s.

ACKNOWLEDGMENT

The authors would like to thank J. Deriso of Trans-Tech Inc., Adamstown, MD, for providing measured data of Fig. 2(b).

REFERENCES

- [1] F. Hernández-Gil and J. Pérez-Martínez, "Analysis of dielectric resonators with tuning screw and supporting structure," *IEEE Trans. Microwave Theory Tech.*, vol. MTT-33, pp. 1453–1457, Dec. 1985.
- [2] F. Hernández-Gil, R. Pérez-Leal, and A. Gebauer, "Resonant frequency stability analysis of dielectric resonators with tuning mechanisms," in *IEEE MTT-S Int. Microwave Symp. Dig.*, Las Vegas, NV, June 1987, pp. 345–348.
- [3] A. Karp, H. J. Shaw, and D. K. Winslow, "Circuit properties of microwave dielectric resonators," *IEEE Trans. Microwave Theory Tech.*, vol. MTT-16, pp. 818–828, Oct. 1968.
- [4] S. Fiedziuszko, "Double dielectric resonator," *IEEE Trans. Microwave Theory Tech.*, vol. MTT-19, pp. 779–781, Sept. 1971.
- [5] S.-W. Chen, K. A. Zaki, and R. G. West, "Tunable temperature-compensated dielectric resonators and filters," *IEEE Trans. Microwave Theory Tech.*, vol. 38, pp. 1046–1052, Aug. 1990.
- [6] C. Wang and K. A. Zaki, "Generalized multilayer anisotropic dielectric resonators," *IEEE Trans. Microwave Theory Tech.*, vol. 48, pp. 60–66, Jan. 2000.
- [7] N. A. McDonald, "Electric and magnetic coupling through small apertures in shield walls of any thickness," *IEEE Trans. Microwave Theory Tech.*, vol. MTT-20, pp. 689–695, Oct. 1972.
- [8] R. Levy, "Improved single and multiaperture waveguide coupling theory, including explanation of mutual interactions," *IEEE Trans. Microwave Theory Tech.*, vol. MTT-28, pp. 331–338, Apr. 1980.
- [9] H.-W. Yao, J.-F. Liang, and K. A. Zaki, "Accuracy of coupling computations and its application to DR filter design," in *IEEE MTT-S Int. Microwave Symp. Dig.*, San Diego, CA, May 1994, pp. 723–726.
- [10] X.-P. Liang and K. A. Zaki, "Modeling of cylindrical dielectric resonators in rectangular waveguides and cavities," *IEEE Trans. Microwave Theory Tech.*, vol. 41, pp. 2174–2181, Dec. 1993.



Tao Shen (S'95) was born in Suzhou, China, in 1969. He is currently pursuing the Ph.D. degree in electrical and computer engineering at the University of Maryland at College Park.



Chi Wang (S'98) received the B.S. and M.S. degrees from Beijing Institute of Technology, Beijing, China, in 1983 and 1986, respectively, and the Ph.D. degree from the University of Maryland, College Park, in 1997, all in electrical engineering.

From 1986 to 1989, he was an Electrical Engineer with the North China Vehicle Research Institute, Beijing. From 1990 to 1992, he was with Beijing New Asia Electronics Inc. He spent one year as a Research Associate at the Beijing Institute of Technology working on modeling of antennas and resonators using the finite difference time-domain method. From 1994 to 1997, he held a Graduate Research Assistantship with Microwave Research Group, University of Maryland at College Park, where he worked on analysis, modeling, and design of microwave circuits and devices. He was a Graduate Teaching Assistant between 1994 and 1995. In 1997, he joined Radio Frequency Systems Inc., where he held several technical positions and is now Engineering Group Manager. He has authored or coauthored more than 40 technical papers in the area of numerical methods and modeling of resonators and filters. His current research interests include new microwave resonator and filter technology, numerical technology, and computer-aided design of advanced RF and microwave circuit for wireless communication systems.



Kawthar A. Zaki (SM'85-F'91) received the B.S. degree (with honors) from Ain Shams University, Cairo, Egypt in 1962 and the M.S. and Ph.D. degrees from the University of California, Berkeley, in 1966 and 1969, respectively, all in electrical engineering.

From 1962 to 1964, she was a Lecturer in the Department of Electrical Engineering, Ain Shams University. From 1965 to 1969, she was a Research Assistant in the Electronics Research Laboratory, University of California, Berkeley. She joined the Electrical Engineering Department, University of Maryland, College Park, in 1970, where she is presently a Professor of electrical engineering. Her research interests are in the areas of electromagnetics, microwave circuits, simulation, optimization, and computer-aided design of advanced microwave and millimeter-wave systems and devices. She has more than 200 publications and five patents on filters and dielectric resonators.

Prof. Zaki has received several academic honors and awards for teaching, research, and inventions.